



Pin groove compressive performance of laminated bamboo lumber at different angles

Haitao Li · Tianyu Gao · Gensheng Cheng ·
Rodolfo Lorenzo

Received: 11 May 2022 / Accepted: 27 October 2022 / Published online: 8 November 2022
© The Author(s), under exclusive licence to Springer Nature B.V. 2022

Abstract In this paper, two kinds of laminated bamboo lumber specimens with 7 groups of fiber angles on plane A and B were designed. The effects of different angles on the compressive strength and stiffness of laminated bamboo lumber were analyzed. According to the test results, the load displacement curves, ultimate strength values and initial stiffness of all specimens were obtained. The compressive strength test values of pin groove based on American Standard 5% diameter offset method were obtained. The results demonstrated that the compressive strength of the pin groove of laminated bamboo lumber obtained by 5% diameter offset method was relatively uniform. The compressive strength of class A pin groove decreased with the increase of angle. The coefficient of variation was within 9.42%, and the standard deviation within 6.33. The compressive strength of class B pin groove first decreased and then increased with the increase of angle. The coefficient of variation was within 12.10%, and the standard deviation within

6.67. The relationship between different fiber angles and the compressive performance of laminated bamboo lumber were analyzed, and the test results were compared with the theoretical formula calculated in the European wood structure and American wood structure design standards. The calculation model of pin groove compressive strength with different fiber angles was put forward.

Keywords Compressive strength of pin groove · Different angles · Laminated bamboo lumber

Introduction

Bamboo grows fast. From the entire process of growth, processing, use and waste treatment, bamboo is a high-quality green building material (Assima et al. 2021; Lei et al. 2021; Su et al. 2021; Li et al. 2022; Zhou et al. 2022). Energy-intensive building materials such as steel, cement and concrete pose a serious threat to the ecological environment and do not meet the basic requirements of green development (Leonel et al. 2022). With the idea of green environmental protection deeply rooted in people, the promotion of green building materials has been the general trend (Li and Lou 2021). China is short of log resources, but rich in bamboo resources. China has the world's most abundant bamboo resources (Wei and Chen 2020), which is distributed in China's 17 provinces cities, autonomous regions south of the

H. Li (✉) · T. Gao · G. Cheng
College of Civil Engineering, Nanjing Forestry University,
Nanjing 210037, China
e-mail: lhaitao1982@126.com

H. Li · T. Gao · G. Cheng
Joint International Research Laboratory for Bio-composite
Building Materials and Structures, Nanjing Forestry
University, Nanjing 210037, China

R. Lorenzo
University College London, London WC1E 6BT, UK

Yangtze River. Bamboo is one of the important forest resources. There are about 78 genera and more than 1400 species of bamboo plants in the world. Bamboo has been widely used as a building material with a long history. Because of its high strength-weight ratio (Rassiah et al. 2013; Li et al. 2019; Zhang et al. 2019; Wang and Shao 2020), bamboo makes its structure light and has good seismic performance (Sassu et al. 2016).

As a kind of engineering bamboo, laminated bamboo lumber has excellently physical and mechanical properties. The bamboo material is used as the basic component in the traditional bamboo structure building in China. Because of the shortcomings of bamboo, such as thin and hollow wall, asymmetrical structure, small diameter, and great variation in geometric size and mechanical properties, the bamboo material cannot be directly applied to the modern bamboo and wood building structure (Sun et al. 2022). Compared with wood, bamboo has short growth cycle, small shrinkage, and high compressive and tensile strength along the grain (Verma and Charriar 2013; Zhou et al. 2019; Lou et al. 2020; Pradhan et al. 2019; Sun et al. 2020; Corbi et al. 2021; Xiao et al. 2021). Many mechanical properties of bamboo can reach the level of wood (Richard and Harries 2015) and can be used as a building structural material instead of ordinary wood (Mahdavi et al. 2011). In recent years, China's bamboo industry has developed rapidly. New products such as bamboo plywood (Qi et al. 2014), bamboo recombination (Yu et al. 2006; Liu et al. 2021), bamboo aggregate (Sharma et al. 2015) and glulam laminated bamboo (Xiao et al. 2014) have been developed with original bamboo as raw material and advanced composite and recombination technology, realizing industrialization. Laminated bamboo lumber is processed into bamboo pieces of fixed width and thickness from fast-growing and short period, and dried to make the moisture content reach 8–12%. After that, bamboo slices are glued together in the same direction into profiles of arbitrary length and cross-section (Li et al. 2016). Laminated bamboo lumber has high mechanical strength, elastic modulus and good machinability. Its tensile strength and compressive strength along the grain can reach 119.19 MPa and 51.41 MPa respectively, corresponding elastic modulus are 10.02 GPa and 8.71 GPa respectively, and the proportional limit is 34.43 MPa (Chen, 2015), which makes up for the

defects of original bamboo. Components of different shapes and sizes can be designed according to actual needs (Xiao et al. 2013), which can meet the requirements of physical and mechanical properties of materials for multi-story building structures. And laminated bamboo lumber is an engineering bamboo with excellently physical properties (Zhou et al. 2012; Chen et al. 2020; Lv et al. 2019; Tian et al. 2019; Wang et al. 2019; Leng et al. 2020; Yang et al. 2020; Mahmud et al. 2021). As a new construction engineering structural material, bamboo not only maintains the characteristics of high strength, good stiffness, wear resistance and low shrinkage rate, but also can easily achieve standardization and modularization of the size of laminated bamboo lumber materials in production (Ferdous et al. 2019).

Joint connection is an important part of bamboo-wood structure. Studies have shown that 80% of the damage of timber structure buildings is caused by the failure of connection joints of timber structure (Itani and Faherty 1984). Therefore, it is very important to study the mechanical properties of bamboo-wood joints. The test of the node is divided into complete node test (Quenneville and Mohammad 2000) and pin groove compressive test (Ramirez et al. 2012). Santos et al. (2010) compared the test methods of complete node test and pin groove compressive test through experimental and numerical research, and believed that the test method had almost no influence on the compressive results, while the pin groove compressive test has the advantages of simplicity, practicality and mass implementation. At present, there are few researches on the influence of different fiber angles on the compressive strength of pin groove. Xu et al. (2019) studied the influence of different angles on the compressive strength of spruce glulam pin groove, and proposed that with the increase of angle, the compressive yield strength of the pin groove decreases first and then increases, and the stiffness gradually decreases. Li (2013) studied the influence of texture angle on the compressive strength and stiffness of the pin groove of recombined bamboo, and found that with the increase of angle, the compressive strength of the pin groove of recombined bamboo first decreased and then increased, and the stiffness showed a significant downward trend. In terms of the theoretical research on the compressive strength of pin groove, the calculation of the relationship between the compressive yield strength and the

fiber angle of laminated bamboo lumber pin groove is rarely involved. In the paper, two modes of laminated bamboo lumber specimens with seven groups of different fiber angles were designed to analyze the influence of different fiber angles on the compressive strength of laminated bamboo lumber pin groove. Through comparing different national standards and the calculated values of modified formula proposed by Xu et al. (2019) and Li (2013), the calculation model of the compressive strength of the pin groove in relation to different fiber angles was put forward, which provided theoretical guidance for the application of laminated bamboo lumber in engineering.

Materials and test methods

Preparation of test materials and specimens

The material used in this test was laminated bamboo lumber, which was produced by Sentai Bamboo and Wood company, Jiangxi province. The raw bamboo was selected from moos bamboo in Yong 'an, Fujian Province. And the unit size of bamboo slice was 2005 mm × 21 mm × 7 mm. Using resorcinol as adhesive, the processed bamboo unit was processed into single layer plate under the main pressure of 9 MPa, side pressure of 6.5 MPa and 157 °C, and then compounded into large section laminated bamboo lumber, as shown in Fig. 1. The steel pin is made of stainless steel with a smooth surface and a diameter of 16 mm.

At present, the test method for measuring the pressure strength of wood pin groove is mainly to make half-hole pin groove pressure bamboo lumped timber specimens according to the requirements of ASTM-D5764 (2013). The height, width and thickness of all specimens were 80 mm, 80 mm and 40 mm, which

were divided into ZLRA and ZLRB categories. When the fiber angle appears on the plane A, it is called class A. The same is true for class B. In the test, the angle between the vertical direction and the fiber was α . In plane A and plane B, there were 7 different angles, 0°, 15°, 30°, 45°, 60°, 75° and 90°, which were parallel to the vertical direction. 10 identical specimens were made for each group. The average density of the specimens was 0.714 g/cm³ and the moisture content was 9%. Detailed drawing and size of specimens were shown in Figs. 2, 3.

Test Method

Design and test loading scheme according to ASTM-D5764 (2013). The experiment was completed in the Structural Laboratory of Civil Engineering Experimental Center of Nanjing Forestry University. The loading equipment is 5 T microcomputer controlled electro-hydraulic servo universal testing machine. The test was controlled by displacement in the whole process with a speed of 1.5 mm/min. The test stopped when the load dropped to 80% of the ultimate load or when the steel pin was embedded in the bamboo and the bamboo at both ends contacted the loading plate. Loading device diagram was shown in Fig. 4.

Test results and analysis

Failure mode

According to the failure characteristics of specimens during the test, 7 groups of ZLRA laminated bamboo lumber specimens with fiber angles of 0°, 15°, 30°, 45°, 60°, 75° and 90° were divided into 4 failure modes. The fiber angle of 0° and 15° is the

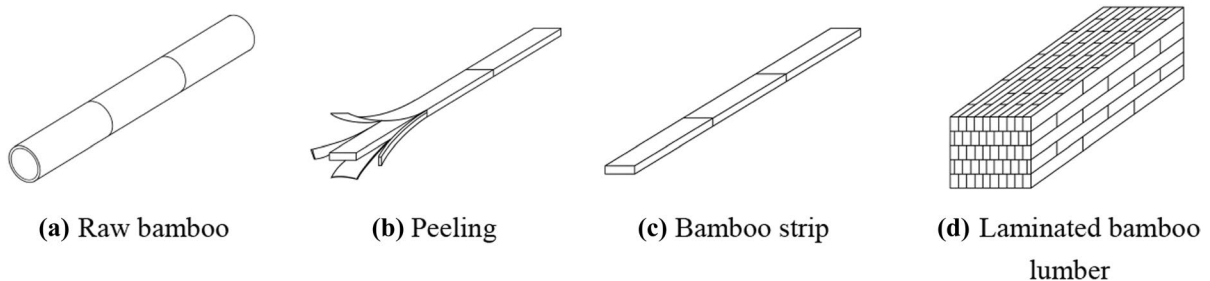


Fig. 1 The production process of laminated bamboo lumber

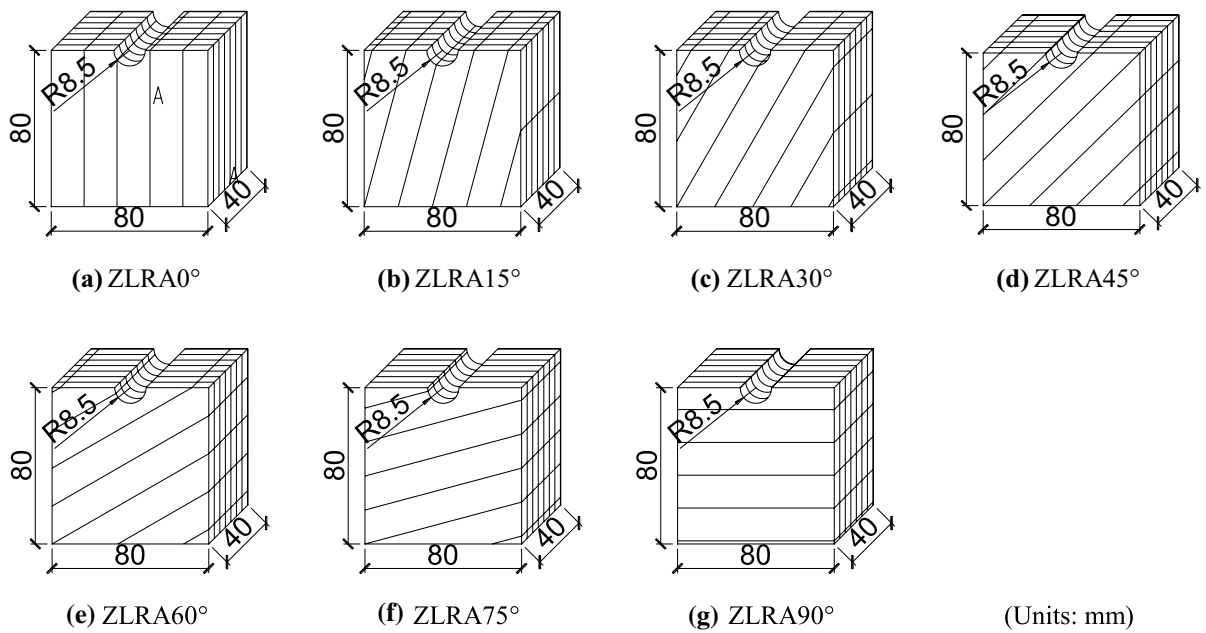


Fig. 2 Detailed drawing of class A texture angle specimen

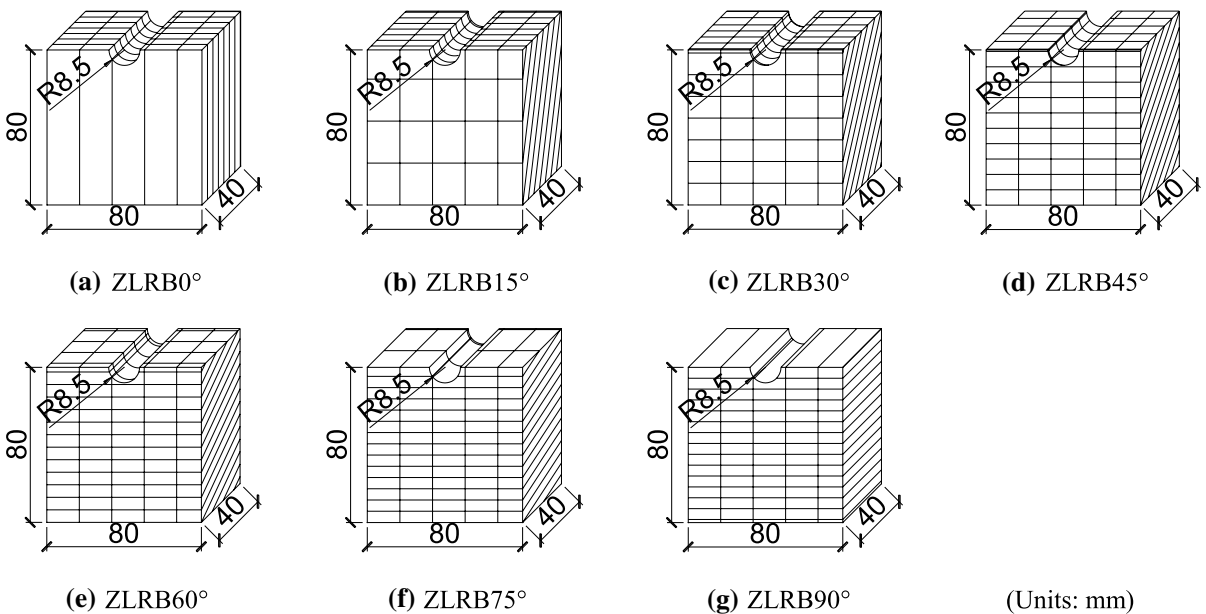
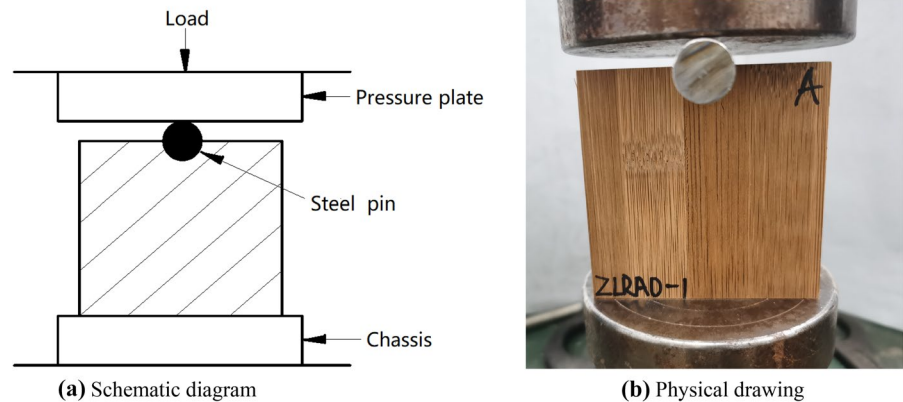


Fig. 3 Detailed drawing of class B texture angle specimen

failure mode I, the fiber angle of 30° and 45° the

failure mode II, the fiber angle of 60° and 75° the

Fig. 4 Pin groove pressure test device diagram



failure mode II, and the fiber angle of 90° the failure mode IV (Figs. 5, 6).

Failure mode I

At the initial stage of test loading, no obvious phenomenon occurred on the specimen surface. As the load increased, it made a hissing sound when the load increased to 20 kN. As the load increased, so did the hiss frequency. Until the load increased to 48 kN, the groove sank, and two vertical cracks close to the horizontal fiber appeared on both sides of the steel pin. The compressive capacity suddenly dropped to 80% of the ultimate load, and the test stopped.

Failure mode II

Laminated bamboo lumber specimens with texture angle of 30° at the initial stage of the test, when the load increased to 23 kN, the specimen made the first hiss sound. As the load increased, the sound was continuous and louder. When the load reached 37 kN, folds appeared near the notch on plane A. When the load reached 40 kN, cracks appeared in the fiber direction. With the increase of load, the crack extended and widened. The failure process of the specimen with the fiber angle of 45° was very similar to that of the specimen with the fiber angle of 30° , both of which were groove sinking, and folds appeared near the groove on plane A. As the angle increased, the notch was seriously damaged. Cracks were also along the direction of the fiber, with the increase of load, continuous extension and widening.

Failure mode III

At the initial stage of loading, starting from 17 kN, the specimens with fiber angle of 60° made a cracking sound. When the load increased to 26 kN, the hole near plane A was destroyed, and the pressure plate continued to decline. The compression deformation of the laminated bamboo lumber specimen was larger than the stroke of the steel pin, so that the pressure plate contacted the upper surface of the specimen, and the test stopped. During the whole process, no cracks occurred on the surfaces of the specimens. The fiber angle was 75° , and the failure process was similar. The steel pin was completely embedded in the specimen, and the groove collapsed, and no cracks appeared on the surface of the specimen.

Failure mode IV

When the fiber angle was 90° , the specimen produced sound from 19 kN. When the load increased to 28 kN, transverse cracks appeared in plane B and D. As the load increased, cracks extended. When the load increased to 35 kN, cracks extended from planes B and D to plane A and C, and then the load decreased to 80% of the ultimate load, and the test stopped.

The failure of ZLRB laminated bamboo lumber specimens could be divided into 4 failure modes. The fiber angle of 0° is the failure mode V, the fiber angle of 15° and 30° the failure mode VI, the fiber angle of 45° , 60° and 75° the failure mode VII, and the fiber angle of 90° the failure mode VIII.

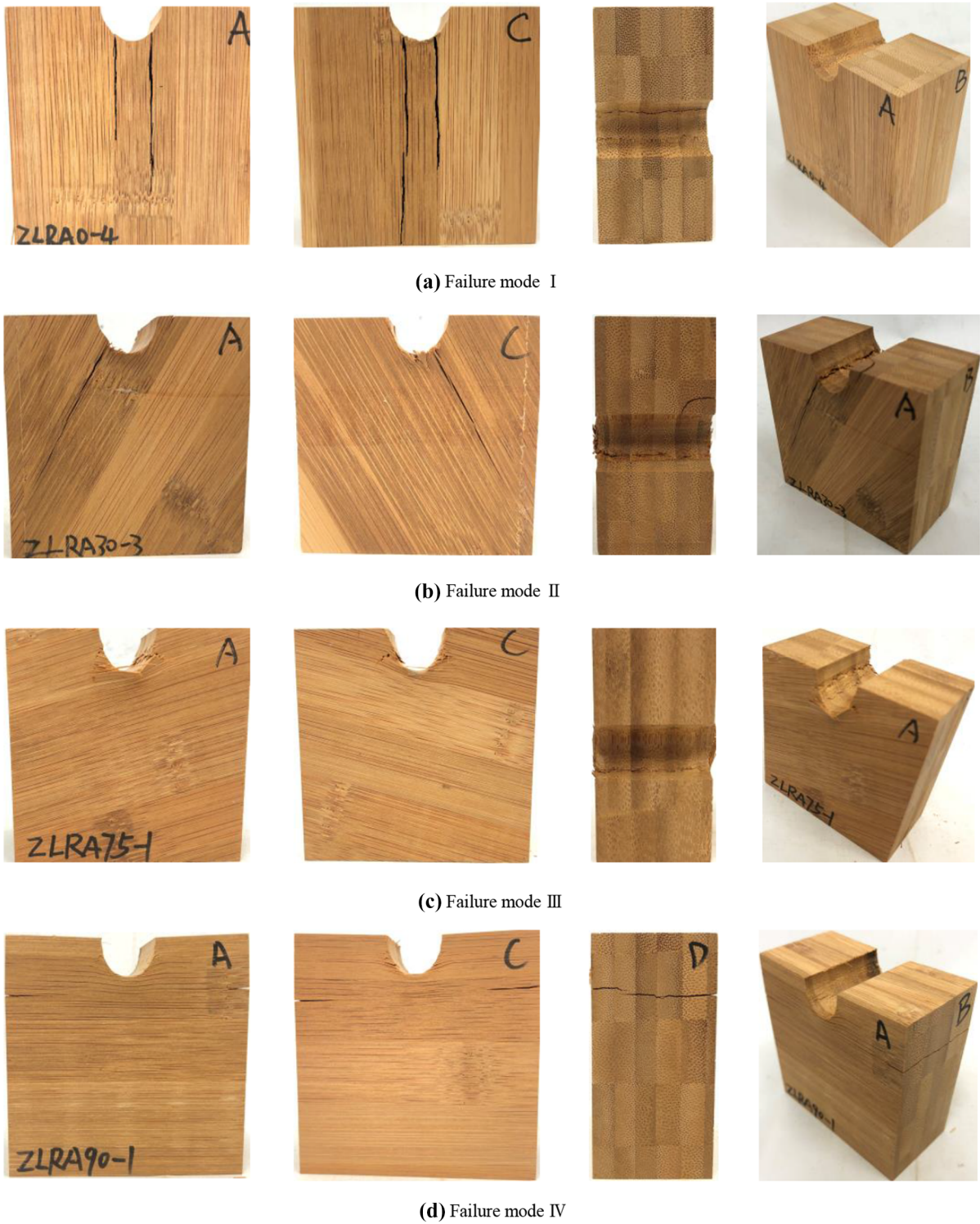


Fig. 5 Failure mode of class A specimen



Fig. 6 Failure mode of class B specimen

Failure mode V

At the initial stage of loading, there was no obvious phenomenon on the surface of the specimen. When the load increased to 21 kN, the specimen began to hiss. With the increasing load, the sound continued and became louder. When the load increased to 40 kN, the slot was crushed, and the load continued to increase. When the ultimate load was 48 kN, two vertical cracks close to the horizontal fiber appeared on both sides of the steel pin, then the load dropped to 80% of the ultimate load, and the test stopped.

Failure mode VI

At the beginning of the test, from 19 kN, the specimen sounded. When the load increased to 37 kN, vertical cracks extending down from the notch along the bonding surface appeared on planes A and C directly below the steel pin. With the increase of load, the notch was crushed, and the cracks continued to extend and widen. When the load increased to 47 kN, it immediately dropped to 80%, and the test stopped.

Failure mode VII

At the initial stage of test loading, the specimen did not change significantly, and at 13 kN, the specimen began to emit a continuous tearing sound. When the load increased to 20 kN, the notch was crushed, and the vicinity of the notch on plane A began to become folded. When the load continued to increase to 25 kN, inclined cracks of the main body almost parallel from the bonding surface suddenly appeared on surfaces A and C, resulting in brittle failure and the end of the test.

Failure mode VIII

With the increase of load, the specimen was compressed, starting from 15 kN, the specimen began to emit continuous sound. When the load reached 23 kN, radial micro-cracks appeared near the slot. With the increase of the load, the cracks extended and expanded. When the load reached 27 kN, inclined

cracks of main body failure suddenly appeared on planes A and C, and the test ended.

Load displacement curve

Figure 7a–g showed the load–displacement curves of class A 7 groups with fiber angles of 0°, 15°, 30°, 45°, 60°, 75° and 90° respectively. At the beginning of the loading process, all specimens underwent an elastic stage, in which the stiffness of each group was relatively stable, and then entered an elastic–plastic stage, in which the stiffness gradually decreased. It could be seen from Fig. 7a–d that when the angle was 0°–45°, the displacement of the steel pin was small and the load dropped. When the compressive capacity dropped to 80% of the ultimate load, the test stopped. It could be seen from Fig. 7e–g that when the angle was 60°–90°, the compression deformation of the specimen was larger than the loading stroke of the steel pin, which made the loading plate contact the specimen surface and stopped the test. The variation trend of load–displacement curve was consistent with the experimental failure phenomenon.

Figure 8a–g respectively showed the load displacement-curves of 7 groups of specimens of class B under load. At the beginning of the loading process, all specimens underwent an elastic stage, and the stiffness of each group was relatively stable, and then entered the elastic–plastic stage, where the stiffness gradually decreased. Figure 8a–c were load–displacement curves of pin groove compressive pressure of specimens with fiber angles of 0°, 15° and 30° respectively. It could be seen that each group of curves was evenly distributed. Basically, with the increase of displacement, its compressive capacity kept increasing, and it could continue to bear greater load when cracks occurred. With the increase of load, cracks continued to expand, the load continued to increase, the bearing capacity of the specimen dropped to 80% of the ultimate load, and the test stopped, belonging to plastic failure.

Figure 8d–g were load–displacement curves of specimens with fiber angles of 45°, 60°, 75° and 90° respectively. It could be seen from the figure that when the load reached a certain load, the compressive capacity of each group of specimens did not increase, and suddenly dropped to 80% of the ultimate load and stopped loading. The reason for the above results was that when the fiber angle was large, the compression

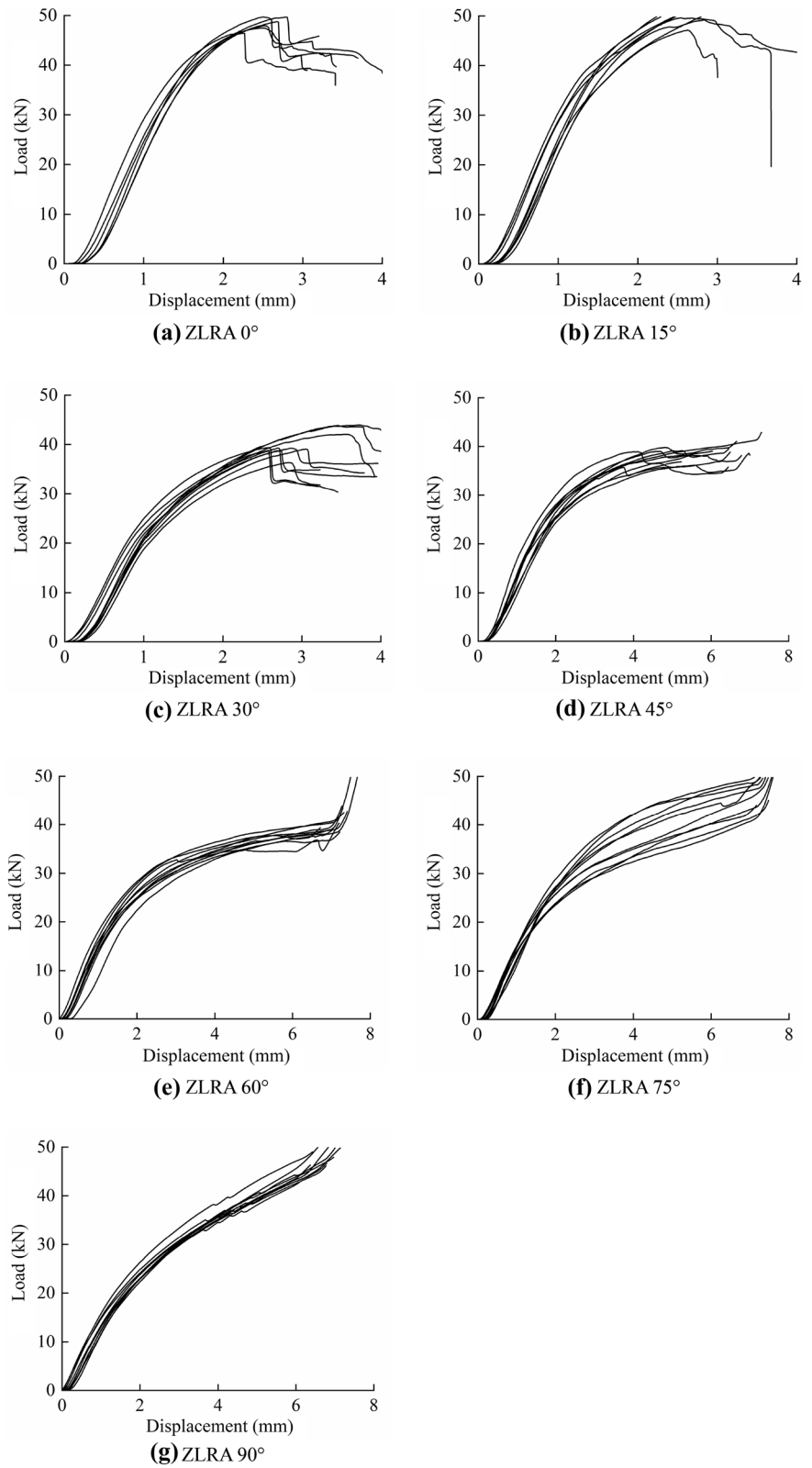
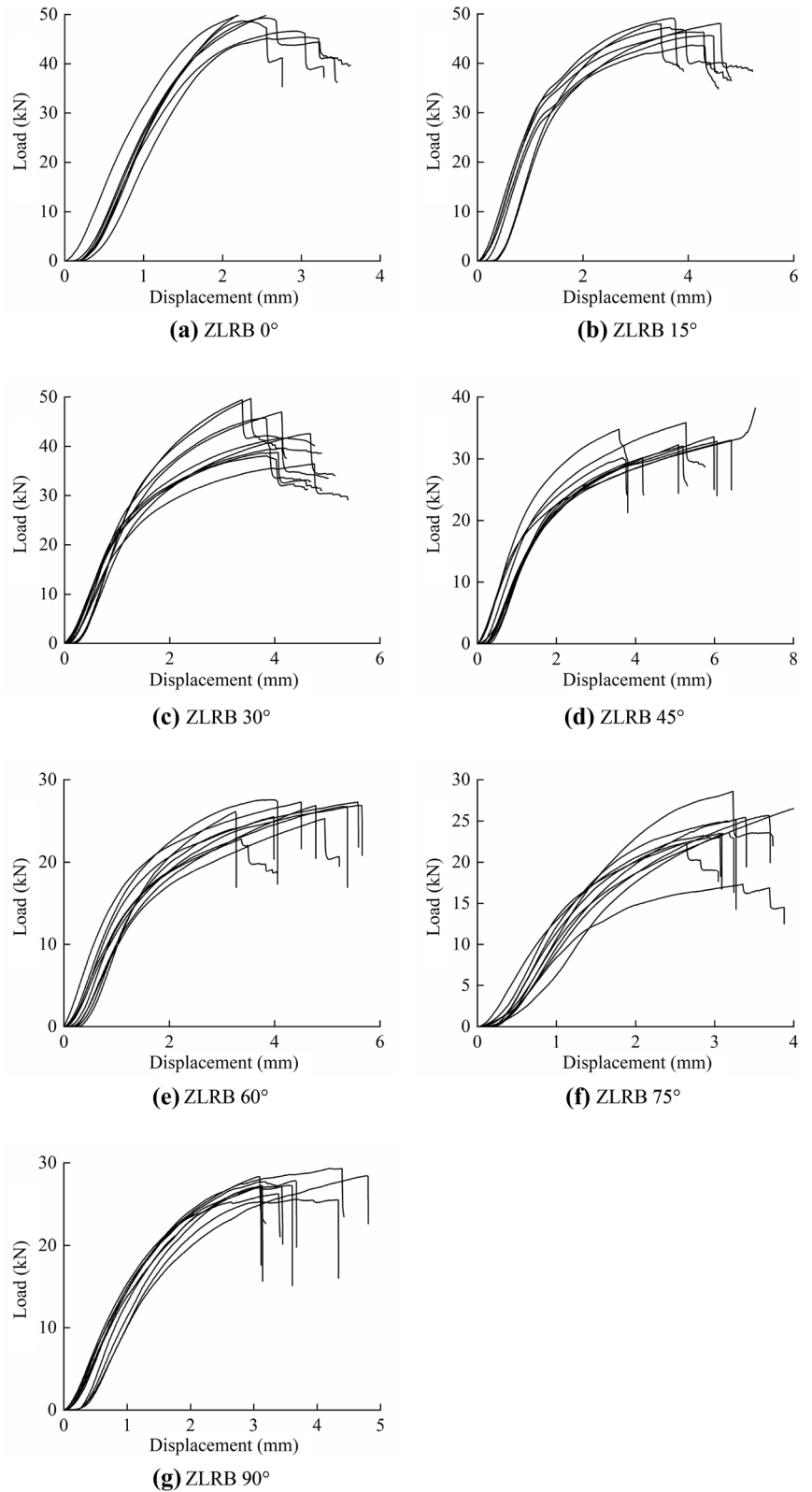
Fig. 7 ZLRA load–displacement curve

Fig. 8 ZLRB load–displacement curve



deformation of the specimen under compression was smaller than the loading stroke of the steel pin. Before the loading plate touched the specimen, large vertical cracks and oblique cracks appeared in the specimen, which made the compressive capacity of the specimen dropped to 80% of the maximum compressive capacity suddenly, and the test stopped. This kind of failure belonged to brittle failure. The variation of load–displacement curve of the specimen was consistent with the failure phenomenon of the specimen.

Comprehensive analysis

Influence of angle on stiffness

It could be seen from Fig. 8 that the stiffness of class A specimen decreased with the increase of angle. There was no significant difference between 0° and 15° groups. When the angle was between 15° and 45°, the initial stiffness decreased with the increase of the angle. When the angle was 45°–90°, the stiffness decreased and gradually became stable. The stiffness of class B specimens decreased first and then increased with the increase of angle. The initial stiffness of the specimens along the grain was the largest, and the initial stiffness was the smallest when the angle was 60°. Similar to class A specimens, there was little difference in stiffness between 0° and 15° groups. When the angle was from 15° to 60°, the stiffness decreased obviously with the increase of the angle. When the angle was between 60° and 90°, the initial stiffness of the specimen showed an increasing trend with the increase of the

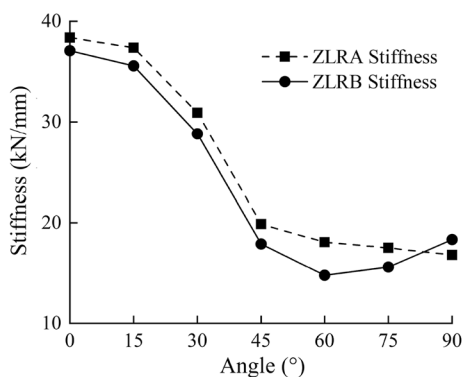


Fig. 9 Stiffness-angle curve

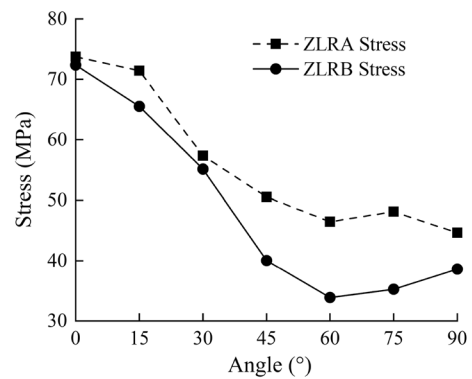


Fig. 10 Stress-angle curve

angle. By comparing the initial stiffness of ZLRA and ZLRB, the initial stiffness of class A texture angle was higher than that of class B texture angle at the same angle, but when the fiber angle was 75°–90°, the stiffness of class B was higher than that of class A in some angle range (Figs. 9, 10).

In order to more accurately compare the relationship between stress and stiffness of ZLRA and ZLRB at the same fiber angle, the data were sorted into Table 1. ZLRA under different angles of the pin groove compressive strength was represented by $f_{5\%,A}$, the stiffness was represented by K_A . ZLRB pin groove compressive strength at different angles was represented by $f_{5\%,B}$, and the stiffness was represented by K_B .

Influence of angle on bearing strength of pin groove

At present, in the pressure test of wood pin groove, pin groove compressive strength values were generally determined by 5% steel pin diameter (5% d) offset method recommended by ASTM-D5764, which had been widely accepted. The stiffness of the specimen in the elastic stage was obtained from the load–displacement curve of the test, and then the inclined line was horizontally shifted according to the 5% d offset method. The vertical coordinate of the intersection of the inclined line and the load–displacement curve was pin groove bearing strength, and the specific value method was shown in Fig. 11.

The strength value can be calculated by the following formula:

Table 1 Pin groove compressive strength and stiffness between ZLRA and ZLRB at different fiber angles

Angle (°)	0	15	30	45	60	75	90
$f_{5\%,A}$ (MPa)	73.78	71.43	57.35	50.54	46.48	48.15	44.63
COV (%)	4.06	3.65	3.96	5.33	4.18	9.11	4.70
SDV (MPa)	3.00	2.61	2.27	2.70	1.94	4.38	2.10
$f_{5\%,B}$ (MPa)	72.37	65.54	55.11	40.03	33.90	35.26	38.60
COV (%)	4.16	8.56	12.10	7.32	7.28	8.87	3.56
SDV (MPa)	3.01	5.61	6.67	2.93	2.47	3.12	1.37
$f_{5\%,A}/f_{5\%,B}$	1.02	1.09	1.04	1.26	1.34	1.37	1.16
K_A (kN/mm)	38.38	37.38	30.90	19.87	18.07	17.51	16.80
COV (%)	8.26	6.29	3.79	16.97	8.10	8.12	6.76
SDV (kN/mm)	3.17	2.35	1.17	3.37	1.46	1.42	1.14
K_B (kN/mm)	37.09	35.58	28.82	17.90	14.77	15.59	18.35
COV (%)	5.06	5.93	10.07	9.92	15.27	14.82	8.43
SDV (kN/mm)	1.88	2.11	2.90	1.78	2.26	2.31	1.55
K_A/K_B	1.03	1.05	1.07	1.11	1.22	1.12	0.92

Number of specimens for class A and class B was 70 respectively. The number of specimens at each angle was 10
 COV coefficient of variation, SDV standard deviation

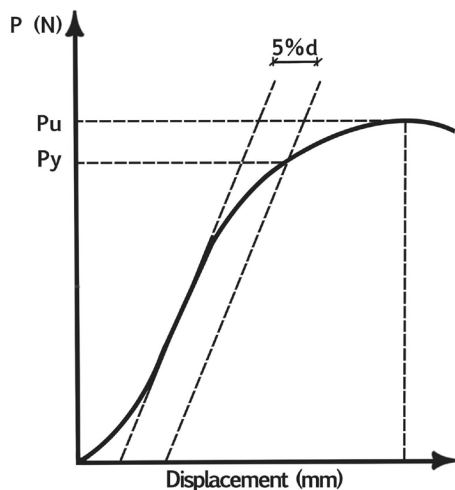


Fig. 11 Value of test yield load

$$f_{5\%} = \frac{P_y}{bt} \tag{1}$$

where $f_{5\%}$ is the compressive strength of 5% diameter offset method pin groove (MPa), P_y is 5% offset load (N), b is the diameter of steel pin (mm), t is the thickness of laminated bamboo lumber specimen (mm).

The formula for calculating the compressive strength of the pin groove at α angle with the grain of wood given in EC5 (2014) is as follows:

$$f_{EC5} = \frac{f_{h,0}}{k_{90} \sin^2 \alpha + \cos^2 \alpha} \tag{2}$$

where $f_{h,0}$ is the pressure strength along the grain pin groove. Soft wood $k_{90}=1.35+0.015 d$, Broadleaf timber $k_{90}=0.90+0.015 d$.

GB/T 50708-2012 (2012) and American Wood Structure Design Standard NDS (2012) give the formula for calculating the compressive strength of pin groove when the angle is α along the grain:

$$f_{NDS,A} = \frac{f_{h,0}f_{h,90}}{f_{h,0} \sin^2 \alpha + f_{h,90} \cos^2 \alpha} \tag{3}$$

where $f_{h,0}$ is the pressure strength along the grain pin groove (MPa), $f_{h,90}$ is the compressive strength of the transverse pin groove (MPa).

GB50005-2017 (2017) gives the strength design value of wood twill pressure according to the following formula:

When $\alpha < 10^\circ$

$$f_{c\alpha} = f_c \tag{4}$$

When $10^\circ < \alpha < 90^\circ$

$$f_{c\alpha} = \frac{f_c}{1 + \left(\frac{f_c}{f_{c,90}} - 1\right) \frac{\alpha - 10}{80} \sin \alpha} \tag{5}$$

where $f_{c\alpha}$ is design value for the strength of wood twill pressure (MPa), α is the angle between the

direction of force and the direction of wood ($^\circ$), f_c is design value for compressive strength of wood along grain (MPa), $f_{c,90}$ is design value for timber transverse grain compressive strength (MPa).

Li (2013) proposed the formula for calculating the compressive strength of the reconstituted bamboo pin groove when it formed α angle with the grain:

When $0^\circ \leq \alpha < 45^\circ$

$$f_\alpha = \frac{f_0 f_{45}}{f_0 \sin^2 \alpha + f_{45} \cos^2 \alpha} \quad (6)$$

When $45^\circ < \alpha \leq 90^\circ$

$$f_\alpha = \frac{f_{45} f_{90}}{f_{45} \sin^2 \alpha + f_{90} \cos^2 \alpha} \quad (7)$$

where f_0 is the design value of the compressive strength of the reconstituted bamboo along the grain (MPa), f_{90} is the design value of transverse compressive strength of reconstituted bamboo (MPa).

Xu et al. (2019) studied the compressive strength of spruce glulam pin groove under different load directions, and put forward the formula for calculating the compressive strength of the pin groove when the load direction is α angle to the wood fiber direction:

$$f_{h,\alpha} = \frac{f_{h,0} f_{h,90}}{f_{h,0} \sin^{1.5} (1.2\alpha) + f_{h,90} \cos^2 \alpha} \quad (8)$$

where $f_{h,0}$ is the design value of grain compression strength of spruce glulam (MPa), $f_{h,90}$ is the design value of transverse compressive strength of spruce glulam (MPa).

In the paper, the compressive strength of pin groove of 0° and 90° laminated bamboo lumber was taken as the reference point, and the formula for calculating the compressive strength of pin groove of laminated bamboo lumber at an α angle with the direction of load was proposed by fitting the test value of strength.

When the load direction was at an α angle with the fiber direction of class A, the formula for calculating the compressive strength of the pin groove of laminated bamboo lumber was as follows:

$$f_{\alpha,5\%,A} = \frac{f_{0,A} f_{90,A}}{f_{0,A} \sin^{1.8} \alpha + f_{90,A} \cos^{1.7} \alpha} \quad (9)$$

where $f_{0,A}$ is the compressive strength value of laminated bamboo lumber along the grain pin groove (MPa), $f_{90,A}$ is the compressive strength of laminated bamboo lumber horizontal grain pin groove (MPa).

When the load direction was at an α angle with the fiber direction of class B, the formula for calculating the compressive yield strength of the pin groove of laminated bamboo lumber was as follows:

$$f_{\alpha,5\%,B} = \frac{f_{0,B} f_{90,B}}{f_{0,B} \sin^2 \alpha + f_{90,B} \cos^{\frac{2}{3}} \alpha} \quad (10)$$

where $f_{0,B}$ is the compressive strength value of laminated bamboo lumber along the grain pin groove (MPa), $f_{90,B}$ is the compressive strength of laminated bamboo lumber horizontal grain pin groove (MPa).

Table 2 presents the statistics of the maximum compressive strength f_{\max} and the compressive strength of 5% diameter offset method $f_{5\%}$. In addition, f_{EC5} is the compressive strength of EC5 (2014),

f_{NDS} is the compressive strength of NDS (2012), $f_{c\alpha}$ is the compressive strength of GB50005-2017 (2017), f_α is the compressive strength of the formula proposed Li (2013), $f_{h,\alpha}$ is the compressive strength of the formula proposed Xu et al. (2019), and $f_{\alpha,5\%}$ is the compressive strength of the formula proposed the paper. In this table, COV is the coefficient of variation, SDV the standard deviation, and δ the error.

Table 2 showed that the formula proposed in the paper was used to calculate the compressive strength of the laminated bamboo lumber pin groove. As you can see, 0° and 15° two sets of pin groove compressive strength of the specimens significantly was greater than other specimen group. The difference was mainly because they were close to parallel fiber compression, in the process of pressure, the specimen along the bonding surface fracturing, most of the rest of the test assembly was splitting and crushing failure mode, which was in line with the damage phenomenon of the specimens.

As can be seen from the data in the Table 2, the theoretical values calculated by the formula recommended by EC5 (2014) were all greater than the experimental values of the compressive strength of the pin groove of laminated bamboo lumber. The theoretical values of the specimens with fiber angles

Table 2 Test and calculated values of compressive strength of laminated bamboo lumber with different fiber angles

Angle (°)	0	15	30	45	60	75	90
$f_{\max,A}$ (MPa)	75.85	76.79	62.63	60.93	67.16	75.74	74.76
COV (%)	2.68	2.43	6.06	5.08	9.42	4.98	4.95
SDV (MPa)	2.03	1.87	3.80	3.09	6.33	3.77	3.70
$f_{5\%,A}$ (MPa)	73.78	71.43	57.35	50.54	46.48	48.15	44.63
COV (%)	4.06	3.65	3.96	5.33	4.18	9.11	4.70
SDV (MPa)	3.00	2.61	2.27	2.70	1.94	4.38	2.10
$f_{\max,B}$ (MPa)	75.76	74.62	65.87	52.05	40.96	38.88	42.92
COV (%)	3.67	4.30	10.04	7.43	5.40	7.43	3.92
SDV (MPa)	2.78	3.21	6.61	3.87	2.21	2.89	1.68
$f_{5\%,B}$ (MPa)	72.37	65.54	55.11	40.03	33.90	35.26	38.60
COV (%)	4.16	8.56	12.10	7.32	7.28	8.87	3.56
SDV (MPa)	3.01	5.61	6.67	2.93	2.47	3.12	1.37
$f_{EC5,A}$ (MPa)	73.78	73.09	71.29	68.95	66.77	65.29	64.72
$\delta_{EC5,A}$ (%)	0	2.32	24.31	36.43	43.65	35.60	45.01
$f_{EC5,B}$ (MPa)	72.37	71.70	69.92	67.64	65.49	64.01	63.48
$\delta_{EC5,B}$ (%)	0	9.40	26.87	68.97	93.48	81.54	64.46
$f_{NDS,A}$ (MPa)	73.78	70.69	63.42	55.62	49.52	45.84	44.63
$\delta_{NDS,A}$ (%)	0	-1.04	10.58	10.05	6.54	-4.80	0
$f_{NDS,B}$ (MPa)	72.37	68.36	59.38	50.35	43.70	39.85	38.60
$\delta_{NDS,B}$ (%)	0	4.30	7.75	25.78	28.91	13.02	0
$f_{c\alpha,A}$ (MPa)	73.78	73.01	68.21	61.38	54.51	48.78	44.63
$\delta_{c\alpha,A}$ (%)	0	2.21	18.94	21.45	17.28	1.31	0
$f_{c\alpha,B}$ (MPa)	72.37	71.61	66.91	60.21	53.47	47.85	43.78
$\delta_{c\alpha,B}$ (%)	0	9.26	21.41	50.41	57.73	34.86	13.42
$f_{\alpha,A}$ (MPa)	73.78	71.57	66.17	47.40	45.97	44.98	44.63
$\delta_{\alpha,A}$ (%)	0	0.20	15.38	-6.21	-1.10	6.58	0
$f_{\alpha,B}$ (MPa)	72.37	68.65	60.21	39.30	38.95	38.69	38.60
$\delta_{\alpha,B}$ (%)	0	4.75	9.25	-1.82	14.90	9.73	0
$f_{h,\alpha,A}$ (MPa)	73.78	60.61	49.33	43.31	41.39	42.89	48.14
$\delta_{h,\alpha,A}$ (%)	0	-15.15	-13.98	-14.31	-10.95	-10.92	7.86
$f_{h,\alpha,B}$ (MPa)	72.37	57.64	45.36	38.81	36.40	37.27	41.64
$\delta_{h,\alpha,B}$ (%)	0	-12.05	-17.69	-3.05	7.37	5.70	7.88
$f_{\alpha,5\%,A}$ (MPa)	73.78	67.78	53.92	51.20	46.57	44.61	44.63
$\delta_{\alpha,5\%,A}$ (%)	0	-5.11	-5.98	1.31	0.19	-7.35	0
$f_{\alpha,5\%,B}$ (MPa)	72.37	65.63	52.53	41.78	33.58	35.54	38.60
$\delta_{\alpha,5\%,B}$ (%)	0	0.13	-4.68	4.37	-0.94	0.79	0

of 0° and 15° were very close to the experimental values, with an error range of 0–9.40%. With the increase of angle, the theoretical value differs greatly from the experimental value, and the error was as high as 93.48%. The theoretical values calculated by NDS (2012) were closer to the experimental values than those calculated by EC5 (2014), and the errors were in the range of -4.80–28.91%. In addition, the error changes of class A and class B had the same

trend, and the error increased first and then decreased with the increase of the angle, indicating that when the fiber angle was large or small, the theoretical value calculated by the formula recommended by NDS (2012) was close to the experimental value. Compared with the experimental value, the theoretical value obtained by the calculation formula of wood twill pressure given in GB50005-2017 (2017) was close to the experimental value when the angle was

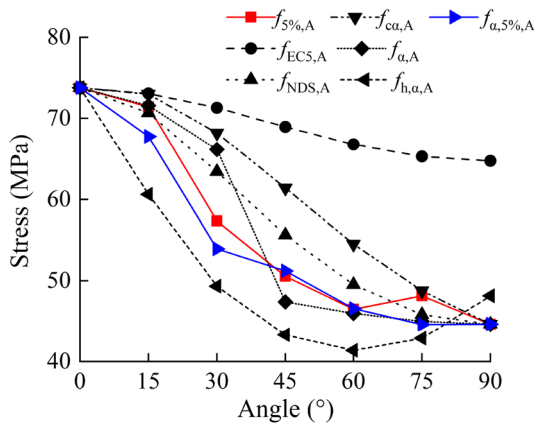


Fig. 12 ZLRA strength-angle curve

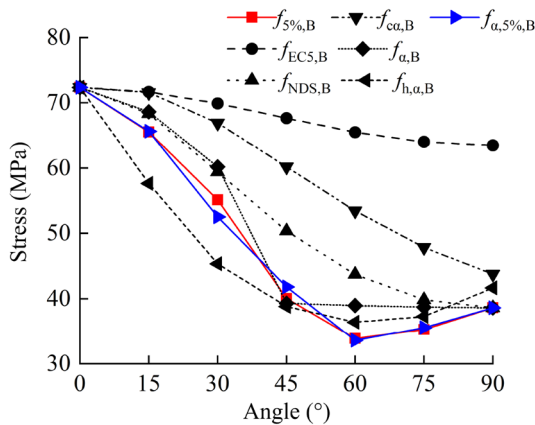


Fig. 13 ZLRB strength-angle curve

15° and 75°, and the errors were 2.21% and 1.31%, respectively. When the angle was 30°, 45° and 60°, the error ranged from 18.94 to 21.54%, and when the angle was 45°, the error reached the maximum 21.54%. For the sample with class B, the difference between the theoretical value and the experimental value was more, and the maximum error could reach 57.73%. The error ranged between the theoretical value and the experimental value was -1.10 – 15.38% through the calculation formula of pin groove compressive pressure proposed by Li (2013). The error ranged between the theoretical value and the experimental value was -17.69 to 7.88% based on the calculation formula of pin groove compressive pressure proposed by Xu et al. (2019). In the paper, the error ranged between the theoretical value and the actual

value calculated by the formula of the compressive strength of the pin groove of laminated bamboo lumber at different angles was -5.98 – 1.31% . Class B fiber angle was -4.63 – 4.37% .

In conclusion, compared with the theoretical values obtained by various specifications and the formulas for pin groove compressive strength with different fiber angles proposed by predecessors, the predicted values obtained by the formulas proposed in this paper were closer to the experimental values. It was in good agreement with the variation trend of the test value of the compressive strength of the pin groove of laminated bamboo lumber in this paper Figures 12, 13.

Conclusion

In this paper, 140 bamboo specimens with 7 groups of different fiber angles of two modes were designed to study the compressive strength of pin groove. 5% diameter offset method was used to obtain the pin groove compressive strength test values of different fiber angles of laminated bamboo lumber. The following conclusions were obtained through analysis:

The relationship between stiffness and fiber angle: with the increase of angle, the initial stiffness of class A specimens gradually decreased. The initial stiffness of class B specimens decreased first and then increased with the increase of angle. The initial stiffness of the members along the grain was the largest, and the initial stiffness was the smallest when the fiber angle was 60°.

The relationship between strength and fiber angle: with the increase of angle, the compressive strength of class A specimens gradually decreased. The compressive strength of class B specimens decreased first and then increased. The compressive strength of the pin groove along the grain was the highest, and the compressive strength was the lowest when the fiber angle was 60°.

In the paper, a formula for calculating the compressive strength of the pin groove of the laminated bamboo lumber was presented. The calculated value was in good agreement with the test value. And the error was in the range of -5.98 – 4.37% , which can ensure the safety and give full play to the strength of the material.

Acknowledgments The writers gratefully acknowledge Ben Chen, Han Zhang, Xiaoyan Zheng, Shaoyun Zhu, Liqing Liu, Dunben Sun, Jing Cao, Yanjun Liu, Junhong Xu and others from the Nanjing Forestry University for helping.

Funding This work was supported by the National Natural Science Foundation of China (No. 51878354 & 51308301); the Natural Science Foundation of Jiangsu Province (No. BK20181402 & BK20130978); 333 talent high-level projects of Jiang-su Province; and Qinglan Project of Jiangsu Higher Education Institutions. Any research results expressed in this paper are those of the writer(s) and do not necessarily reflect the views of the foundations.

Declarations

Conflict of interest The authors declare that they have no conflicts of interest to this work.

References

- American National Standards Institute (2012) National design specification for wood construction: NDS-2015. Washington, D.C.: American Forest and Paper Association
- American Society for Testing and Materials (2013) Standard test method for evaluating dowel-bearing strength of wood and wood-based products: ASTM D5764–97. West Conshohocken: ASTM
- Assima D, Haitao L, Zhenhua X, Rodolfo L (2021) A review of mechanical behavior of structural laminated bamboo lumber. *Sustain Struct* 1(1):000004. <https://doi.org/10.54113/j.sust.2021.000004>
- British Standards Institution (2014) BS EN 1995-1-1: 2004+A2: 2014. Eurocode 5: design of timber structures—Part 1–1: General—Common rules and rules for buildings.
- Chen G, Jiang H, Yu YF, Zhou T, Li X (2020) Experimental analysis of nailed LBL-to-LBL connections loaded parallel to grain. *Mater Struct* 53(4):1–13. <https://doi.org/10.1617/s11527-020-01517-5>
- Chen W (2015) Mechanical properties analysis and experimental study of laminated bamboo lumber unidirectional bias component. Southeast University
- Corbi O, Baratta A, Corbi I, Tropeano F, Liccardo E (2021) Design issues for smart seismic isolation of structures: past and recent research. *Sustain Struct* 1(1):000001. <https://doi.org/10.54113/j.sust.2021.000001>
- Ferdous W, Bai Y, Ngo TD, Manalo A, Mendis P (2019) New advancements, challenges and opportunities of multi-storey modular buildings—A state-of-the-art review. *Eng Struct* 183:883–893
- Ministry of Construction, PRC (2017) GB 50005-2017, Standard for design of timber structures
- Ministry of Construction, PRC (2012) GB/T 50708–2012, Technical code of glued laminated timber structures
- Itani R Y, Faherty K F (1984) Structural wood research: state-of-the-art and research needs. ASCE
- Lei W, Zhang Y, Yu W, Yu Y (2021) The adsorption and desorption characteristics of moso bamboo induced by heat treatment. *J Renewable Mater* 6(3):41–46. <https://doi.org/10.13360/j.issn.2096-1359.202009024>
- Leng Y, Xu Q, Harries KA, Chen L, Liu K, Chen X (2020) Experimental study on mechanical properties of laminated bamboo beam-to-column connections. *Eng Struct* 210:110305. <https://doi.org/10.1016/j.engstruct.2020.110305>
- Leonel M, Rodolfo L, Li H (2022) An innovative digital workflow to design, build and manage bamboo structures. *Sustain Struct* 2(1):000011. <https://doi.org/10.54113/j.sust.2022.000011>
- Li YJ, Lou ZC (2021) Progress of bamboo flatten technology research. *J for Eng* 6(4):14–23. <https://doi.org/10.13360/j.issn.2096-1359.202012021>
- Li H, Zhang Q, Wu G, Xiong X, Li Y (2016) A review on development of laminated bamboo lumber. *Journal of Forestry Engineering* 1(6):10–16
- Li H, Qiu Z, Wu G, Wei D, Lorenzo R, Yuan C (2019) Compression behaviors of parallel bamboo strand lumber under static loading. *J Renewable Mater* 7(7):583–600. <https://doi.org/10.32604/jrm.2019.07592>
- Li H, Chen B, Fei B, Xiong Z, Lorenzo R, Ashraf M (2022) Mechanical properties of aramid fiber reinforced polymer confined laminated bamboo lumber column under cyclic loading. *Eur J Wood Wood Prod* 80:1057–1070. <https://doi.org/10.1007/s00107-022-01816-4>
- Li X Z (2013) Research on bearing performance of bolt joint for recombinant bamboo. Chinese Academy of Forestry, Beijing, China
- Liu J, Zhou AP, Sheng BL, Liu YY, Sun LW (2021) Effect of temperature on short-term compression creep property of bamboo scrimber. *J for Eng* 6(2):64–69. <https://doi.org/10.13360/j.issn.2096-1359.202006003>
- Lou ZC, Yang LT, Zhang AW, Shen D, Liu J, Yang L, Li Y (2020) Influence of saturated steam heat treatment on the bamboo color. *J for Eng* 5(4):38–44
- Lv Q, Ding Y, Liu Y (2019) Study of the bond behaviour between basalt fibre-reinforced polymer bar/sheet and bamboo engineering materials. *Adv Struct Eng* 22(14):3121–3133
- Mahdavi M, Clouston PL, Arwade SR (2011) Development of laminated bamboo lumber: review of processing, performance, and economical considerations. *J Mater Civ Eng* 23(7):1036–1042. [https://doi.org/10.1061/\(ASCE\)MT.1943-5533.0000253](https://doi.org/10.1061/(ASCE)MT.1943-5533.0000253)
- Mahmud A, Mohammad JH, Safat A (2021) Semi-rigid behaviour of stainless steel beam-to-column bolted connections. *Sustain Struct* 1(1):000002. <https://doi.org/10.54113/j.sust.2021.000002>
- Pradhan NPN, Paraskeva TS, Dimitrakopoulos EG (2019) Quasi-static reversed cyclic testing of multi-culm bamboo members with steel connectors. *Journal of Building Engineering* 27:100983. <https://doi.org/10.1016/j.jobbe.2019.100983>
- Qi JQ, Xie JL, Huang XY, Yu WJ, Chen SM (2014) Influence of characteristic inhomogeneity of bamboo culm on mechanical properties of bamboo plywood: effect of culm height. *J Wood Sci* 60(6):396–402. <https://doi.org/10.1007/s10086-014-1429-8>
- Quenneville JHP, Mohammad M (2000) On the failure modes and strength of steel-wood-steel bolted timber connections

- loaded parallel-to-grain. *Can J Civ Eng* 27(4):761–773. <https://doi.org/10.1139/100-020>
- Ramirez F, Correal JF, Yamin LE, Atoche JC, Piscal CM (2012) Dowel-bearing strength behavior of glued laminated *Guadua* bamboo. *J Mater Civ Eng* 24(11):1378–1387. [https://doi.org/10.1061/\(ASCE\)MT.1943-5533.0000515](https://doi.org/10.1061/(ASCE)MT.1943-5533.0000515)
- Rassiah K, Ahmad MMHM, Ali A (2013) Mechanical properties of laminated bamboo strips from *Gigantochloa Scortechinii* polyester composites. *Mater Des* 57:551–559. <https://doi.org/10.1016/j.matdes.2013.12.070>
- Richard MJ, Harries KA (2015) On inherent bending in tension tests of bamboo. *Wood Sci Technol* 49(1):99–119
- Santos CL, De Jesus AMP, Morais JLL, Lousada JLPC (2010) A comparison between the EN 383 and ASTM D5764 test methods for dowel-bearing strength assessment of wood: experimental and numerical investigations. *Strain* 46(2):159–174
- Sassu M, De Falco A, Giresini L, Puppio ML (2016) Structural solutions for low-cost bamboo frames: experimental tests and constructive assessments. *Materials* 9(5):346. <https://doi.org/10.3390/ma9050346>
- Sharma B, Gatóo A, Bock M, Ramage M (2015) Engineered bamboo for structural applications. *Constr Build Mater* 81:66–73. <https://doi.org/10.1016/j.conbuildmat.2015.01.077>
- Su J, Li H, Xiong Z, Lorenzo R (2021) Structural design and construction of an office building with laminated bamboo lumber. *Sustain Struct* 1(2):000010. <https://doi.org/10.54113/j.sust.2021.000010>
- Sun X, He M, Li Z (2020) Novel engineered wood and laminated bamboo lumbers for structural applications: State-of-art of manufacturing technology and mechanical performance evaluation. *Constr Build Mater* 249:118751. <https://doi.org/10.1016/j.conbuildmat.2020.118751>
- Sun H, Li X, Li H, Hui D, Gaff M, Lorenzo R (2022) Nanotechnology application on bamboo material: a review. *Nanotechnol Rev* 11:1670–1698. <https://doi.org/10.1515/ntrev-2022-0101>
- Tian L, Kou Y, Hao J (2019) Axial compressive behaviour of sprayed composite mortar–original laminated bamboo lumber columns. *Constr Build Mater* 215:726–736. <https://doi.org/10.1016/j.conbuildmat.2019.04.234>
- Verma CS, Chariar VM (2013) Stiffness and strength analysis of four layered laminate laminated bamboo lumber at macroscopic scale. *Compos B* 45(1):369–376. <https://doi.org/10.1016/j.compositesb.2012.07.048>
- Wang F, Shao Z (2020) Study on the variation law of bamboo fibers' tensile properties and the organization structure on the radial direction of bamboo stem. *Ind Crops Prod* 152:112521. <https://doi.org/10.1016/j.indcrop.2020.112521>
- Wang X, Zhou A, Zhao L, Chui YH (2019) Mechanical properties of wood columns with rectangular hollow cross section. *Constr Build Mater* 214:133–142. <https://doi.org/10.1016/j.conbuildmat.2019.04.119>
- Wei X, Chen FM, Wang G (2020) Flexibility characterization of bamboo slivers through winding-based bending stiffness method. *J for Eng* 5(2):48–53
- Xiao Y, Yang RZ, Shan B (2013) Production, environmental impact and mechanical properties of glulam. *Constr Build Mater* 44:765–773. <https://doi.org/10.1016/j.conbuildmat.2013.03.087>
- Xiao Y, Shan B, Yang RZ, Li Z, Chen J (2014) Glue laminated bamboo (Glulam) for structural applications *Materials and Joints in timber structures*. Springer, Dordrecht, pp 589–601
- Xiao F, Wu Y, Zuo Y, Peng L, Li W, Sun X (2021) Preparation and bonding performance evaluation of bamboo veneer/foam aluminum composites. *J for Eng* 6(3):35–40. <https://doi.org/10.13360/j.issn.2096-1359.202009024>
- Xu X, Teng Q, Que Z, Zhang L (2019) Influence of different load directions on bearing strength of spruce glulam pin groove. *Build Technol* 50(04):419–422
- Yang D, Li H, Xiong Z, Mimendi L, Lorenzo R, Corbi I, Hong C (2020) Mechanical properties of laminated bamboo under off-axis compression. *Compos A* 138:106042. <https://doi.org/10.1016/j.compositesa.2020.106042>
- Yu W, Yu Y, Zhou Y, Ren DH (2006) Studies on factors influencing properties of reconstituted engineering timber made from small-sized bamboo. *China for Prod Ind* 33(6):24–28
- Zhang T, Wang A, Wang Q, Guan F (2019) Bending characteristics analysis and lightweight design of a bionic beam inspired by bamboo structures. *Thin-Walled Struct* 142:476–498. <https://doi.org/10.1016/j.tws.2019.04.043>
- Zhou A, Huang D, Li H, Su Y (2012) Hybrid approach to determine the mechanical parameters of fibers and matrixes of bamboo. *Constr Build Mater* 35:191–196. <https://doi.org/10.1016/j.conbuildmat.2012.03.011>
- Zhou H, Wang G, Chen L, Yu Z, Smith LM, Chen F (2019) Hydrothermal aging properties of three typical bamboo engineering composites. *Materials* 12(9):1450. <https://doi.org/10.3390/ma12091450>
- Zhou K, Li H, Dauletbek A, Yang D, Xiong Z, Lorenzo R, Corbi O (2022) Slenderness ratio effect on the eccentric compression performance of chamfered laminated bamboo lumber columns. *J Renewable Mater* 10(1):165–182. <https://doi.org/10.32604/jrm.2021.017223>

Publisher's Note Springer Nature remains neutral with regard to jurisdictional claims in published maps and institutional affiliations.

Springer Nature or its licensor (e.g. a society or other partner) holds exclusive rights to this article under a publishing agreement with the author(s) or other rightsholder(s); author self-archiving of the accepted manuscript version of this article is solely governed by the terms of such publishing agreement and applicable law.